

LATTICE BOLTZMANN METHOD AND DIFFUSION IN MATERIALS WITH LARGE DIFFUSIVITY RATIOS

by

Edouard WALTHER*, **Rachid BENNACER**, and **Caroline DE SA**

LMT, ENS Cachan, University Paris-Saclay, France

Original scientific paper
<https://doi.org/10.2298/TSCI141027206W>

This work is centered on the safe usage of the lattice Boltzmann method for 2-D pure diffusion. The basics of the method for pure diffusion are first elucidated using a new definition given in the paper. The oscillating behavior and safe conditions of use are then explored in the case of homogeneous material as well as heterogeneous materials with circular and plane interfaces. As a conclusion, the range of valid relaxation factors is given for a correct use of lattice Boltzmann method.

Key words: *lattice Boltzmann, diffusion, diffusivity ratio, oscillations, D_2Q_5 , D_2Q_9*

Introduction

The lattice Boltzmann method (LBM) is an explicit and locally formulated method for solving the Navier-Stokes equation [1]. It is also suited for diffusion problems in homogeneous or heterogeneous media, with a high parallelization potential [2]. The LBM shows interesting features as well for the numerical simulation of phase-change [3]. However, in this case the implementation is not straightforward and the algorithm does not stay fully explicit at every stage [4].

The literature about the LBM and its stability range is abundant [1, 5, 6]. Demuth *et al.* [7] explore the performance of LBM for diffusion simulation *vs.* classical methods, in terms of precision for various imposed gradient conditions and for large diffusivity ratios. However, they do not mention how to overcome the problem of oscillation rising when the relaxation factors are close to their boundary values. This problem is brightly solved by [8], using a fictitious isotropic advection velocity to simulate diffusion coefficients in heterogeneous media with diffusive properties reaching several orders of magnitude.

There is nevertheless a range of relaxation factors where the LBM can be used safely without having to modify the scheme or using artifacts such as [8]. To the best of our knowledge, no authors have been publishing their observations regarding the behavior of the method at the extrema of the relaxation factors, be it for homogeneous materials or for heterogeneous ones, considering in this case variations of the diffusion coefficient.

This work intends to fill this lack for the use of non-experts LBM programmers and will hence focus on presenting the numerical results regarding oscillations when Dirichlet boundary conditions are imposed on both homogeneous and heterogeneous materials with various geometries.

* Corresponding author, e-mail: edouard.walther@ens-cachan.fr

Lattice Boltzmann method for pure diffusion

This section shows the basics of the LBM used for pure diffusion in homogeneous and heterogeneous media.

Homogeneous media case

The LBM is a mesoscopic approach that can fit the macroscopic phenomena governed by partial derivative equations problems. The evolution of a fluid or a solid is deduced from the consideration of a population of particles interacting with well-defined rules of collision. Unlike the well-known Navier-Stokes approach that uses the equations describing the macroscopic behavior of a fluid and then discretizes them to the microscopic level, the LBM is an *ascendant* method, where the particles agitation defined by the Maxwell-Boltzmann distribution of statistical mechanics allows for a consistent extrapolation towards the macroscopic behavior. The link between micro and macroscopic scales is reached thanks to a Chapman-Enskog expansion [1].

Practically, for mass or thermal diffusion or for flow problems, the LBM consists in considering a population of particles streaming along given directions in the space systematically on the points of the grid. The particles displacement is chosen equal to unity in every direction, hence the time and space scales are strongly linked. At each time step, the particles

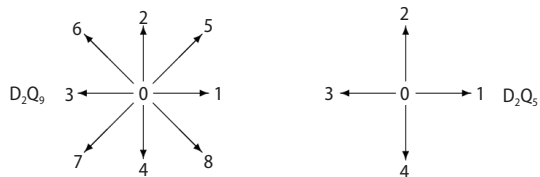


Figure 1. Arrows showing the directions of propagation of the D_2Q_9 and the D_2Q_5 stencils

distributions stream to their neighboring nodes (orthogonally and/or diagonally) and exchange their energy by collision. Figure 1 gives an example of distribution propagation for the D_2Q_9 and D_2Q_5 models, where subscript 2 represents the dimension of space, 9 and 5 being the number of discrete distributions streaming on the grid (the sum of the possible space directions).

Boltzmann's equation ruling the particles behavior is given under following form, f being the density of probability of the particles, c – the speed of propagation, and Ω – the collision operator:

$$\frac{\partial f}{\partial t} + c \nabla f = \Omega(f) \quad (1)$$

After discretizing the space into D_2Q_9 , as previously defined, with $0 \leq k \leq 8$ and $c_k = 1$ *lattice unit per time step in direction* as the mesoscopic speed of the particle on the grid, one obtains:

$$\frac{\partial f_k}{\partial t} + c_k \frac{\partial f_k}{\partial x_k} = \Omega_k \quad (2)$$

In the Bhatnagar-Gross-Krook approach [5], the collision operator is approximated as a relaxation of the distribution function towards the equilibrium distribution:

$$\Omega_k = -\frac{1}{\tau} (f_k - f_k^{\text{eq}}) \quad (3)$$

The equilibrium distribution function f_k^{eq} of eq. (3) is computed through the Taylor expansion of the Maxwell-Boltzmann distribution of a stationary perfect gas at the equilibrium, which, for the diffusion process, simplifies merely:

$$f_k^{\text{eq}} = \omega_k \rho \quad (4)$$

The ρ factor is the sum of the distributions at the point considered and represents the computed macroscopic value, e. g. the concentration or temperature of the simulated matter. The factor ω_k is a constant weighting relative to the propagation direction, such that $\sum \omega_k = 1$. Long displacements are less likely than short ones, hence the decreasing weightings of zero displacement, orthogonal displacement, and diagonal displacement for the D_2Q_9 scheme.

Setting out $\omega = \Delta t/\tau$ and writing the Boltzmann equation with its discrete form, one obtains the explicit equation of the space-time evolution of the f_k functions:

$$f_k(x + \Delta x, t + \Delta t) = f_k(x, t) - \omega [f_k(x, t) - f_k^{\text{eq}}(x, t)] \quad (5)$$

For stability reasons [1, 5], the ω factor has to remain strictly between 0 and 2. In the case of 2-D diffusion in a single given medium, the relationship between ω and the LBM diffusivity, d , is:

$$d = c_s^2 \left(\frac{1}{\omega} - \frac{1}{2} \right) \quad (6)$$

In eq. (6), $c_s = 1/(3)^{1/2}$ is a parameter called the sound speed in LBM space-time, but is actually only a scaling factor in the case of diffusion [9].

In order to make a LBM simulation with a given number of time steps, t_{LBM} , and a mesh size, N , correspond with the evolution, t_{real} , of a real domain, L , one has to make their Fourier numbers match:

$$F_o = \frac{d t_{\text{LBM}}}{N^2} = \frac{D t_{\text{real}}}{L^2} \quad (7)$$

In eq. (7), D is the thermal diffusivity of the real medium. Changing the LBM diffusivity or refining the mesh will hence affect the number of time steps to be computed [5]. For more details about LBM and its boundary conditions, see [10].

Taking the explicit finite differences method (FDM) as a reference for comparison, one can see on fig. 2(a) the evolution of the error ratio between LBM and FDM for an equal discretization, as well as the ratio of time steps required for both methods to simulate a given timespan. The horizontal dashed line is the unity ratio which provides a reference for the amount of time steps required for LBM compared to the explicit FDM, [11]. The LBM is also more precise than FDM for almost any value of the relaxation factor, except $\omega = 0$.

From fig. 2(a), one can conclude that the relaxation factor shall be small enough to be competitive vs. classical methods, ideally below the unity ratio, yet big enough to allow for a sufficient precision of the method vs. a classical one such as FDM.

The precision of the 5- and 9-velocities models were also compared vs. the pure diffusion analytical solution of *semi-infinite wall* for a defined simulation time corresponding to $F_o = 0.01$. The results in terms of maximum and average relative error are plotted vs. the relaxation factor on fig. 2(b). Both models have similar orders of magnitude of error, the D_2Q_9 one being slightly more precise. The maximum relative error reaches $\sim 10^{-20}\%$ for $\omega = 0$, and the minimum relative error is below $10^{-60}\%$ at a value of $\omega \sim 1.1$. Noticeably the relative error curve has the same shape for any Fourier simulation time and the ω corresponding to the minimum error value increases towards with the increase of the Fourier number.

Having laid the foundations of LBM simulation of diffusion in homogeneous media, the application of this method to heterogeneous requires a simple adaptation, as explained in the following section.

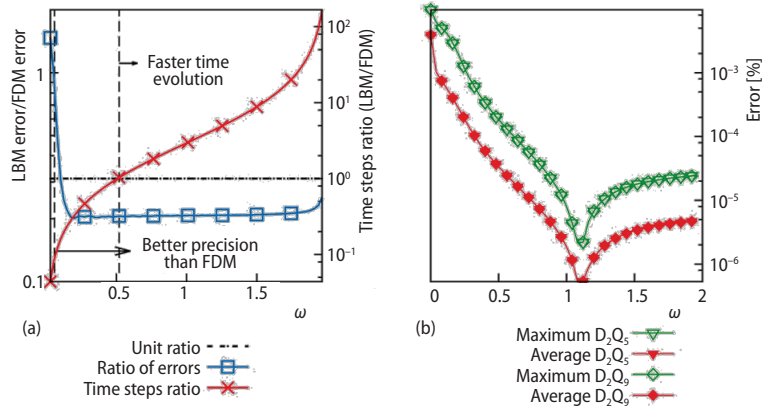


Figure 2. Comparison of the precision and performance of LBM vs. the FDM (a) and relative error of the method vs. the analytical semi-infinite wall solution (b)

Heterogeneous media case

Regarding the simulation of diffusion in two materials *a* and *b*, the best practice is to define a relaxation factor for one of them as presented in eq. (6) and then determine the value of the other one depending on the ratio of real diffusivities:

$$\frac{d_a}{d_b} = \frac{D_a}{D_b}$$

$$\omega_b = \frac{1}{\left(\frac{d_b}{c_s^2} + \frac{1}{2}\right)}$$

From this relationships between the physical properties of the materials, one can plot the relationship from ω_a to ω_b , as presented on fig. 3. This graph shows the strong dependency of the relaxation factor of the second material with the diffusivity ratio. The experience shows however that for heterogeneous media with a diffusivity ratio reaching several orders of magnitude, some perturbations appear at boundaries or at the interfaces between phases,

which is the topic of next section.

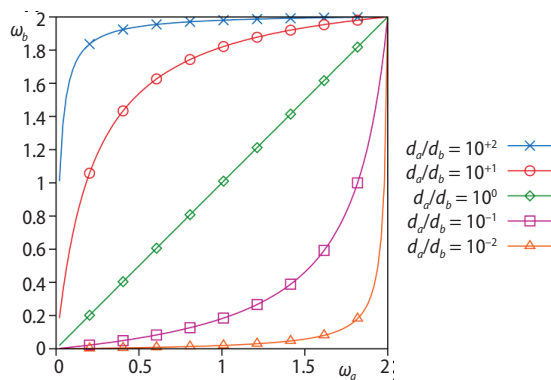


Figure 3. Relationship between ω_a and ω_b for diffusivity ratios with several orders of magnitude

Oscillating behavior of D₂Q₅ and D₂Q₉ stencils

The aim of this section is to provide a guideline for LBM users that do not wish to modify their code, introducing a fictitious advection velocity as in [8]. First, a definition for the phenomenon of oscillation is proposed. The oscillatory behavior of both 5- and 9-velocities stencils is then confronted to geometries with increasing complexity. Eventually, a test on a realistic cementitious morphology completes the study.

Definition

Under the term *oscillations* we understand the existence or the conjunction of following events:

- Transient appearance of values without the range of the physically imposed gradient (*e. g.* obtaining a negative value for a 0-1 imposed scalar range). These non-physical values vanish over time.
- Fluctuating scalar values with changing sign at a given point of the mesh whereas the imposed gradient does not change.
- Fluctuating scalar values at a given point of the mesh, whereas the imposed gradient does not change

The word *stable* in this work is hence not to be understood in the generally used sense of numerical stability but as qualifying the behavior of LBM regarding oscillations.

Oscillations for homogeneous media

For homogeneous media, oscillations appear for higher values of the relaxation factor. Figure 4 presents the couples (D , ω) for which we obtained non-physical values at early time steps after imposing a scalar gradient to the considered 200×200 pixels domain. Both the D_2Q_9 and D_2Q_5 stencils are appropriate when using relaxation factors below $\omega \sim 1.2$.

Using higher relaxation factors with the aim of increasing the methods precision (as shown in fig. 2) appears to be counter-productive, as for higher relaxation factors, oscillations show up at early time steps, fig. 4.

The relative amplitude of these oscillations reaches $\sim 10\%$ of the imposed gradient, as plotted on the second vertical axis of fig. 4. The relative values of oscillations are steadily increasing with ω , however they are damped over time and vanish after a sufficient amount of time steps, as presented on fig. 4.

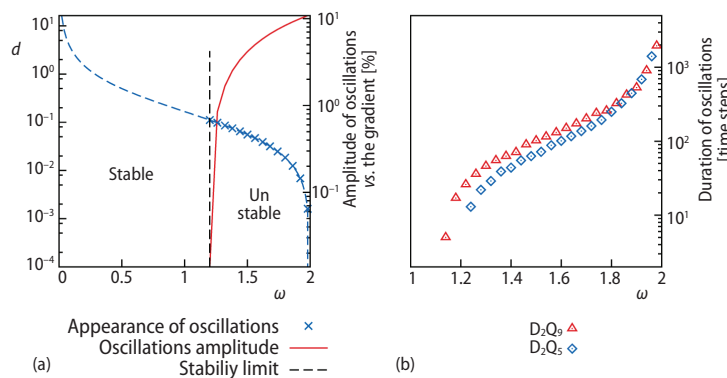


Figure 4. Oscillations limit and number of time steps required for a complete damping of oscillations for the D_2Q_9 and D_2Q_5 stencils; homogeneous media, square geometry (200×200 pixels)

Oscillations for heterogeneous media

Following the rules set by eqs. (8) and (9), several configurations of 200×200 pixels heterogeneous material with varying diffusivity ratios and different geometries are examined in this section. The reference relaxation factor ω_a is affected to the grey domain on all plots.

Serial association

Numerical investigations were led on a regular bi-material, with a unity gradient applied orthogonally to the interface (*e. g.* from the top to the bottom of fig. 5). As this situation is similar to the homogeneous one, the same features can be found in terms of non-oscillating zone with a clearly defined maximum relaxation factor.

For both schemes, some oscillations appear at very low relaxation factors and diffusivity ratios below 0:1 for a number of time steps close to half the size of the mesh, fig 5. This phenomenon is due to the time required by the streaming process for collisions to take place at the interface between the materials. When the particles reach the interface, they collide with other particles having a much smaller relaxation factor, whence the oscillations.

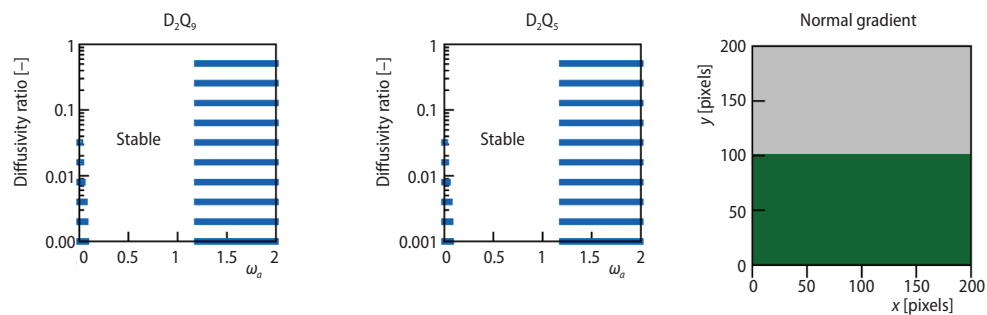


Figure 5. Oscillations for various diffusivity ratios in the case of heterogeneous media with an orthogonal gradient to the interface, square geometry (200×200 pixels)

For D_2Q_5 and D_2Q_9 , defining a relaxation factor such as $0.1 < \omega_a < 1.2$ allows for a safe use of LBM for any diffusivity ratio in this configuration, which can be of peculiar interest for the simulation of diffusion in materials associated in series.

Parallel association

The tests performed with an interface-parallel gradient showed a tighter zone of safe use of the D_2Q_9 stencil, fig. 6. The oscillations appear at the very first time steps on nodes at each side of the interface near the imposed scalar boundary for this scheme. The condition to be respected is hence $0.1 < \omega_a < 1$.

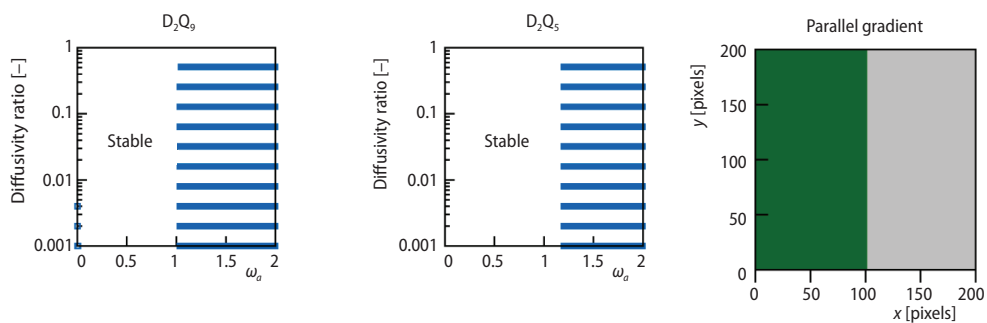


Figure 6. Oscillations for various diffusivity ratios in the case of heterogeneous media with gradient direction along the interface, square geometry (200×200 pixels)

The 5-velocities model is unaffected by the parallel association, which implies a sensitivity of the diagonal terms to the variation of relaxation factor.

Inclined geometries

The same simulations with a the same top-to-bottom unity gradient in the y-axis direction were lead on three geometries with decreasing slopes. The results shown on figs. 7-9 show that both stencils have a similar behavior, the D_2Q_9 one being the more restrictive.

Remarkably, for the 1:1 slope, the diagonal distributions of D_2Q_9 are parallel to the isovalues in some zones of the domain. They are hence unaffected by the geometry which translates into a bigger stable zone compared to the 1:2 and 1:4 slopes, fig. 7.

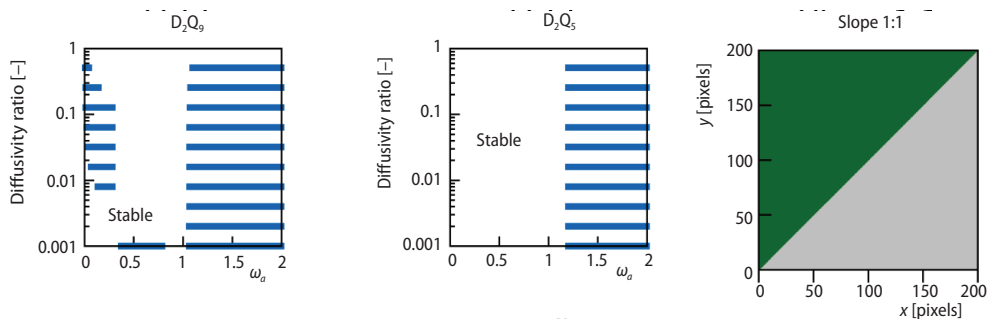


Figure 7. Oscillations for various diffusivity ratios in the case of heterogeneous media with north/south gradient direction, slope 1:1, square geometry (200 × 200 pixels)

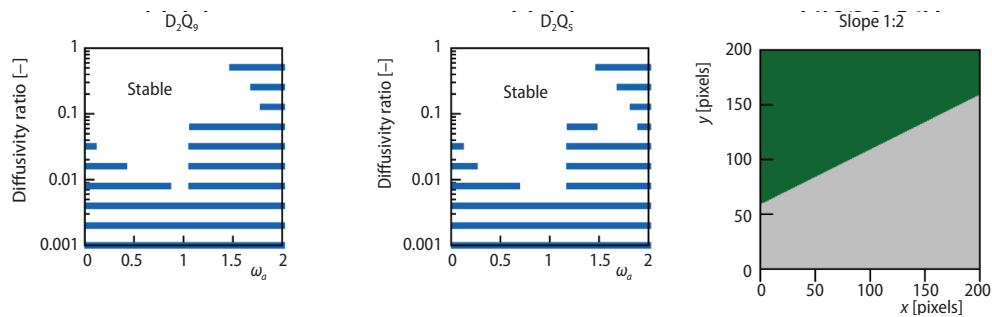


Figure 8. Oscillations for various diffusivity ratios in the case of heterogeneous media with north/south gradient direction, slope 1:2, square geometry (200 × 200 pixels)

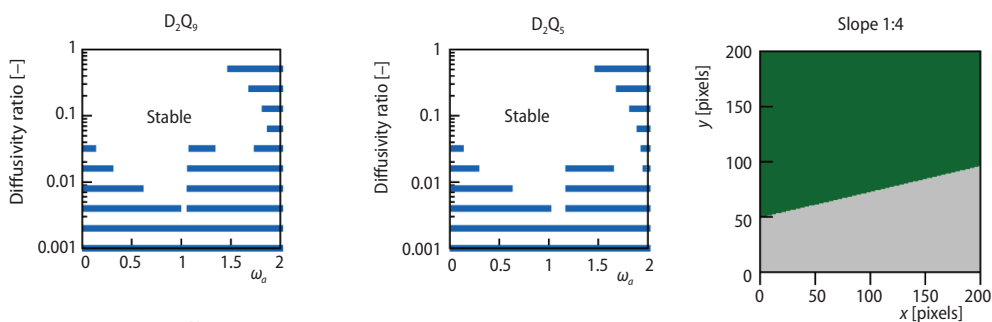


Figure 9. Oscillations for various diffusivity ratios in the case of heterogeneous media with north/south gradient direction, slope 1:4, square geometry (200 × 200 pixels)

The D_2Q_5 stability zone for the 1:1 slope configuration, fig. 7, has exactly the same shape as the normal gradient configuration, fig. 5.

For both models, the stability zone increases slightly as the slope decreases. This behavior is expected indeed, when the slope approaches 0, the material association tends towards the serial association.

Inclusions in the matrix

Three circular inclusions with increasing radius in a matrix are considered in this section. The reference relaxation factor is affected to the inclusion material. The loci of oscillations for increasing inclusion fractions are illustrated on figs. 10-12.

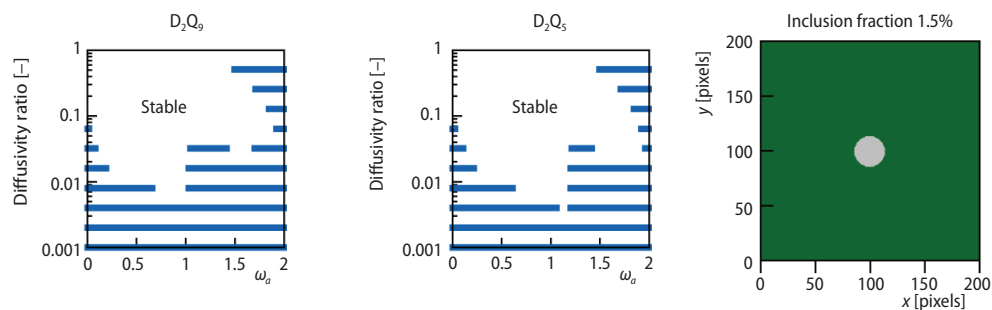


Figure 10. Oscillations for various diffusivity ratios in the case of a cylindrical inclusion with 1.5% fraction (200×200 pixels mesh)

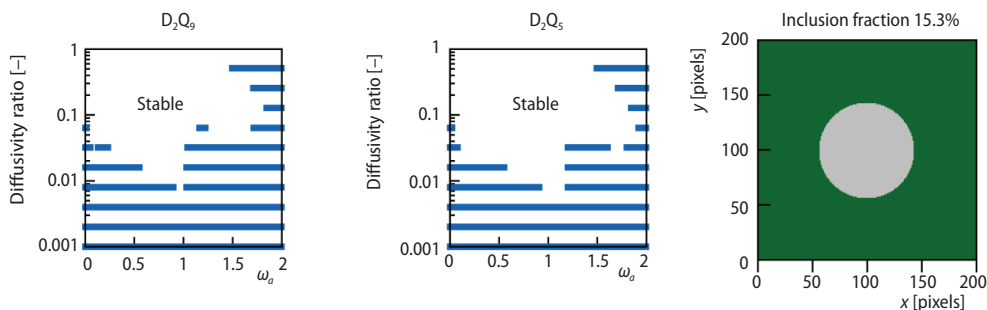


Figure 11. Oscillations for various diffusivity ratios in the case of a cylindrical inclusion with 15.3% fraction (200×200 pixels mesh)

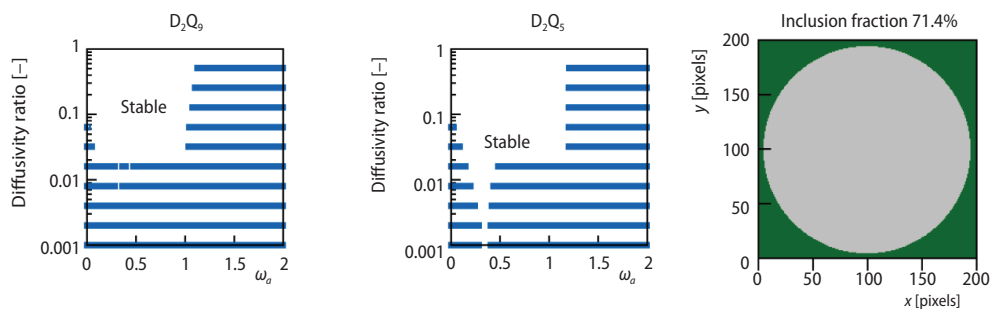


Figure 12. Oscillations for various diffusivity ratios in the case of a cylindrical inclusion with 71.4% fraction (200×200 pixels mesh)

Interestingly, the shape of the stability zones for circular inclusion is very likely to the one of the 1:2 slope and 1:4 slope configurations.

From this study, one can conclude that the higher the inclusion surface, the smaller the stability zone (both for D_2Q_5 and D_2Q_9).

Cementitious paste-like morphology

For this numerical test, the same morphological scheme as in [12] was used to reconstruct cementitious-resembling matter. Both schemes have a rather stable behavior for such matter, the shape of the stability zones being a more restrictive version of the homogeneous one, fig. 13.

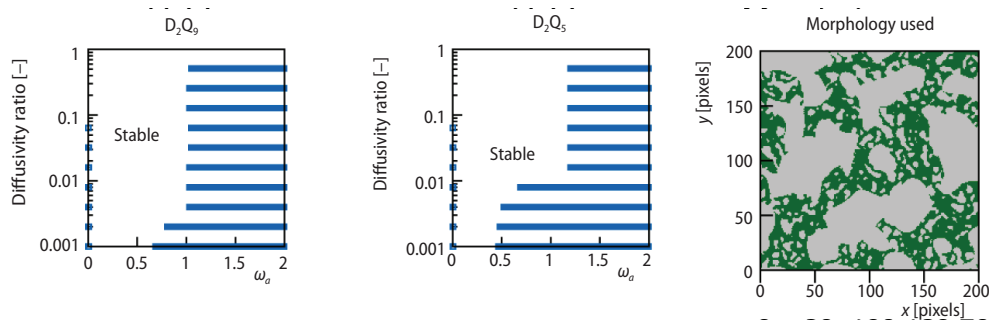


Figure 13. Oscillations for various diffusivity ratios in the case of cementitious-like reconstructed matter (200 × 200 pixels mesh)

Conclusions

This work shows the range of relaxation factors that allow for a safe use for simple geometries. Care has to be taken when using high diffusivity ratios as oscillations are very likely to appear for more complex geometries. Imposing a relaxation factor having several orders of magnitude is indeed equivalent to forcing a discontinuity in a partial differential equation, which leads to numerical oscillations.

The choice of the ω relaxation factor has an influence on the required amount of time steps for a given physical time, as well as on the precision of the method and on the possible appearance of oscillations which, although they may disappear once the static regime is reached, induce an error for the simulation of transient systems.

Materials with sufficiently weak diffusivity differences, id est ratios of 0:6 or above, are not subject to causing oscillations. Also, for complex structures having diffusivity ratios above two orders of magnitude, no oscillations appear if the correct ω is chosen. To reduce both the error introduced by the oscillations at low relaxation factors and to be at the *right side* from the ω value giving a minimum, *i. e.* where the relative error has an asymptotic behavior, fig. 2(b), one should run simulations of diffusion in heterogeneous materials with the highest possible ω . Giving the highest relaxation factor to the material having the biggest surface fraction is also advised for the same purposes.

Nomenclature

c	– particle velocity, [ms^{-1}]	d	– the LBM diffusivity, [-]
c_k	– discrete particle velocity in direction, [$= (\text{lattice dimension}) \cdot (\text{lattice time})^{-1}$]	F_o	– Fourier number, [-]
c_s	– the LBM pseudo-speed of sound, [$= (\text{lattice dimension}) \cdot (\text{lattice time})^{-1}$]	f	– distribution function of the particles, [-]
D	– mass or thermal diffusivity, [m^2s^{-1}]	f_k	– discrete distribution function in direction k , [-]
		t	– time, [s]

Greek symbols

ρ	– macroscopic quantity, e. g., [°C]	ω	– relaxation factor, [–]
τ	– collision frequency, [(lattice unit) ⁻¹]	ω_a, ω_b	– relaxation factor of material <i>a</i> and <i>b</i> , [–]
Ω	– collision operator, [–]	ω_k	– discrete collision operator in direction <i>k</i> , [–]

References

- [1] Mohamad, A. A., *Lattice Boltzmann Method – Fundamentals and Engineering Applications with Computer Codes*, Springer Edition, New York, USA, 2011
- [2] Walther, E., *et al.*, Cement Paste Morphologies and Effective Diffusivity: Using the Lattice Boltzmann Method, *European Journal of Environmental and Civil Engineering*, 19 (2015), 10, pp. 1-13
- [3] Ganaoui, M. El., Semma, E. A., A Lattice Boltzmann Coupled to Finite Volumes Method for Solving Phase Change Problems, *Thermal Science*, 13 (2009), 2, pp. 205-216
- [4] Jourabian, M., *et al.*, Lattice Boltzmann Simulation of Melting Phenomenon with Natural Convection from an Eccentric Annulus, *Thermal Science*, 17 (2013), 3, pp. 877-890
- [5] Wolf-Gladrow, D. A., *Lattice-Gas Cellular Automata and Lattice Boltzmann Models – An Introduction*, Springer, New York, USA, 2000
- [6] Servan-Camas, B., Tsai, F.-T.-C., Non-Negativity and Stability Analyses of Lattice-Boltzmann Method for Advection-Diffusion Equation, *Journal of Computational Physics*, 228 (2008), 1, pp. 236-256
- [7] Demuth, C., *et al.*, Performance of Thermal Lattice Boltzmann and Finite Volume Methods for the Solution of Heat Conduction Equation in 2D and 3D Composite Media with Inclined and Curved Interfaces, *International Journal of Heat and Mass Transfer*, 77 (2014), Oct., pp. 979-994
- [8] Perko, J., Patel, R. A., Single-Relaxation-Time Lattice Boltzmann Scheme for Advection-Diffusion Problems with Large Diffusion-Coefficient Heterogeneities and High-Advection Transport, *Physica Review*, 89 (2014), 5, pp. 053309-9
- [9] Nourgaliev, R. R., *et al.*, The Lattice Boltzmann Equation Method: Theoretical Interpretation, Numerics and Implications, *International Journal of Multiphase Flow*, 29 (2003), 1, pp. 117-169
- [10] Ziegler, D. P., Boundary Conditions for Lattice Boltzmann Simulations, *Journal of Statistical Physics*, 71 (1993), 1, pp. 1171-1177
- [11] Walther, E., *et al.*, Lattice Boltzmann Method Applied to Diffusion in Restructured Heterogeneous Media, *Defect and Diffusion Forum*, 354 (2014), June, pp. 237-242
- [12] Roubin, E., *et al.*, Multi-Scale Failure of Heterogeneous Materials: a Double Kinematics Enhancement for Embedded Finite Element Method, *International Journal of Solids and Structures*, 52 (2014), Jan., pp. 180-196